JACS
JOURNAL OF THE AMERICAN CHEMICAL SOCIETY

Article

pubs.acs.org/JACS

Disaccharides Impact the Lateral Organization of Lipid Membranes

Gemma Moiset,[†] Cesar A. López,[†] Rianne Bartelds,[†] Lukasz Syga,[†] Egon Rijpkema,[†] Abhishek Cukkemane,[‡] Marc Baldus,[‡] Bert Poolman,*[,†] and Siewert J. Marrink*[,†]

[†]Groningen Biomolecular Sciences and Biotechnology Institute and Zernike Institute for Advanced Materials, University of Groningen, Nijenborgh 7, 9747 AG Groningen, The Netherlands

[‡]NMR Spectroscopy, Bijvoet Center for Biomolecular Research Department of Chemistry, Faculty of Science, Utrecht University, Padualaan 8, 3584 CH Utrecht, The Netherlands

Supporting Information

ABSTRACT: Disaccharides are well-known for their membrane protective ability. Interaction between sugars and multicomponent membranes, however, remains largely unexplored. Here, we combine molecular dynamics simulations and fluorescence microscopy to study the effect of mono- and disaccharides on membranes that phase separate into L_o and L_d domains. We find that nonreducing disaccharides, sucrose and trehalose, strongly destabilize the phase separation leading to uniformly mixed membranes as opposed to monosaccharides and reducing disaccharides. To unveil the driving force for this process, simulations were performed in which the sugar linkage was artificially modified. The availability of accessible interfacial binding sites that can accommodate the nonreducing disaccharides is key for their strong impact on lateral membrane organization. These exclusive interactions between the nonreducing sugars and the membranes may rationalize why organisms such as yeasts, tardigrades, nematodes, bacteria, and plants accumulate sucrose and trehalose, offering cell protection under anhydrobiotic conditions. The proposed mechanism might prove to be a more generic way by which surface bound agents could affect membranes.

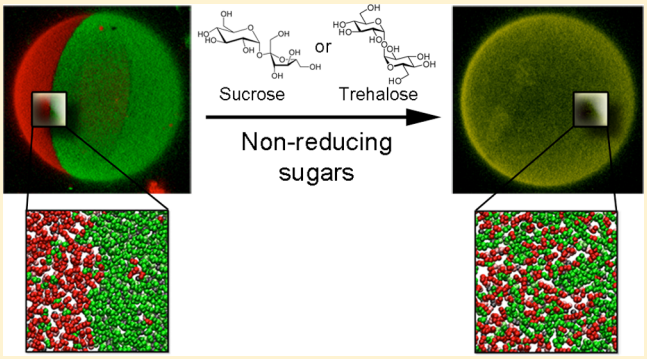

INTRODUCTION

One of the most intriguing phenomena in biology is the occurrence of anhydrobiosis in the life cycle of several organisms from all kingdoms of life such as yeasts, tardigrades, nematodes, bacteria, and plants. In the anhydrobiotic state, the amount of liquid water in the organism is reduced to a level where the metabolism is completely (but reversibly) stopped.[1−3] A common physiological response to anhydrobiosis is the synthesis of cryo-protective sugars, such as the disaccharides sucrose (by plants) and trehalose (mostly by animals), which are accumulated intracellular also during temperature drifting, osmotic shifting, and oxidative stress.[4,5] The role of those nonreducing sugars in the protection against the dehydration damage is not fully understood. However, they have been shown to stabilize protein conformations and lipid bilayers.[6]

The direct interaction between lipid and sugar molecules has been demonstrated by a diversity of experimental techniques, including infrared spectroscopy, differential scanning calorimetry, nuclear magnetic resonance (NMR), and X-ray diffraction.[7−12] Sugars have proven to be effective in protecting membranes by lowering the gel−fluid phase transition upon dehydration. This phenomenon has been observed for the monosaccharide glucose and the disaccharides sucrose and trehalose.[13−15] The effect can be explained by a direct replacement of the water molecules by the sugars, preventing the increase in the packing of the lipid acyl chains in the dry state. This effect is called the "water replacement" hypothesis.[16−18] Other explanations for the protection ability of sugars during dehydration are the "vitrification", the "water-entrapment", and the "hydration repulsion" hypotheses, which indicate that sugars protect biomolecules by the formation of amorphous glasses, by concentrating water molecules close to the membrane, or by being excluded from the surface.[19−21] The latter would reduce the compressive stress of the membrane upon dehydration. Even though different hypotheses have been put forward, several studies have indicated that different mechanisms of protection may act simultaneously.[18]

In fully hydrated membranes, the nature of sugar−lipid interactions is debated, and they have been classified on the basis of either "interaction" or "exclusion" hypotheses. In the first one, the sugars interact directly with the lipid membranes as seen by an expansion of the phospholipid monolayers when sucrose or trehalose is added.[22−25] The increased membrane area is caused by the sugars intercalating between the lipid headgroups. On the contrary, the "exclusion" hypothesis describes a partial depletion of sugar in the hydration zone of

Received: June 7, 2014
Published: October 14, 2014

   dx.doi.org/10.1021/ja505476c | J. Am. Chem. Soc. 2014, 136, 16167−16175

the lipid bilayer.[11,13,21,25] Andersen and co-workers demonstrated that the two opposing views on lipid–sugar interactions might both be true and take place simultaneously. At low sugar concentration the attractive contribution between sugar and lipid by hydrogen bonding dominates, resulting in the intercalation of the sugars in between the lipid headgroups. At higher concentrations the interface saturates, and kosmotropic contributions dominate, causing a general depletion of additional sugars from the interface.[25]

So far, studies have been mostly directed at simplified model membranes. Real membranes, however, consist of a complex mixture of hundreds of different lipid types and proteins. The current view describes biomembranes as a heterogeneous material in which preferential association of certain lipids, sterols, and proteins can lead to the formation of nanodomains, so-called "lipid rafts". Such rafts, enriched in cholesterol and saturated lipids, display physicochemical properties different from those of their disordered fluid surroundings, and they are believed to play an important role in the self-assembly of membrane proteins into functional platforms.[26,27] Thus, a complete overview of the mechanism of action of different sugars should be analyzed and compared in terms of membranous lateral heterogeneity.

In this work we have used molecular dynamics (MD) simulations together with fluorescence confocal microscopy to study the effects of sugars on membranes with coexisting liquid-ordered (L_o) and liquid-disordered (L_d) domains, a prototypical raft-mimicking model system. We find that the lateral organization of the membrane is affected by the interaction with small sugars. Single monosaccharides (glucose and fructose) and reducing disaccharides (including palatinose, maltose, and gentiobiose) do not affect coexisting L_o and L_d phases, while nonreducing disaccharides (e.g., trehalose and sucrose) disrupt the domains and promote lipid remixing, resulting in more vesicles with a single phase of mixed lipids.

RESULTS

Liquid-Ordered Domains Dissolve When Coated with Disaccharides in Computer Simulations. To probe the effect of sugars on phase-separated membranes, we modeled a ternary membrane system composed of dipalmitoylphosphatidylcholine (DPPC), dilinoleylphosphatidylcholine (DLiPC), and cholesterol (4:3:3 molar ratio), which is laterally partitioned into two coexisting fluid domains: a L_o domain rich in saturated lipids (DPPC) and cholesterol, and a L_d domain containing a high amount of the polyunsaturated lipid (DLiPC) and a reduced level of cholesterol. We performed MD simulations of this system at a coarse-grained (CG) level of resolution, using the Martini force field.[28]

Figure 1A shows the CG topology for the different lipid and sugar molecules simulated, together with the starting structure of the system. In the absence of sugars, the domain separation is stable, in line with the experimental phase diagram for similar ternary mixtures.[29] However, after the addition of 200 mM of sucrose, we observe a clear destabilization of the L_o and L_d domains as illustrated in the graphical snapshots from the simulation (Figure 1B). To quantify the mixing of the lipid constituents, the fraction of contacts between the saturated and unsaturated lipids was calculated (Figure 1C). The number of contacts steadily increases during the simulation, pointing to a destabilizing effect of sucrose on the domains. Toward the end of the simulation, after 2 μs, an almost homogeneously mixed membrane is observed. The mixing process seems to occur very

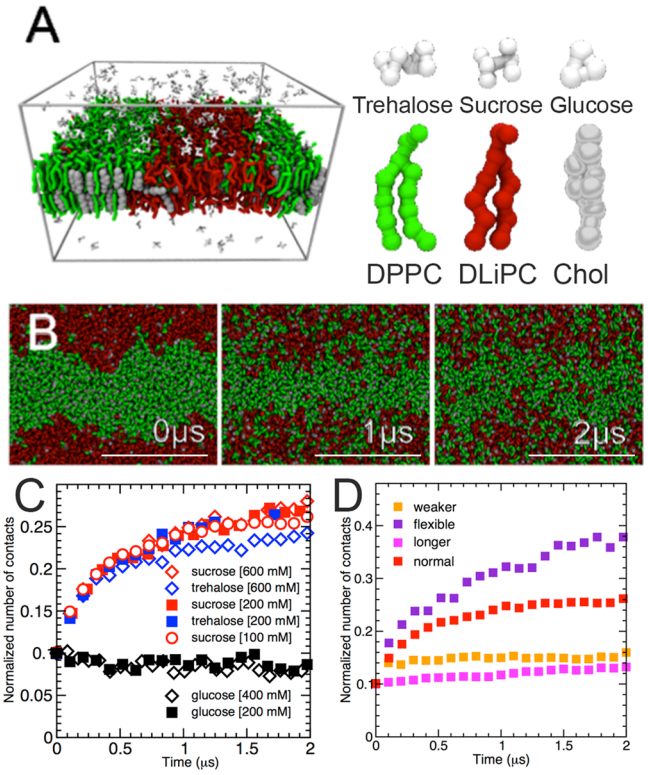

Figure 1. Domain mixing induced by disaccharides. (A) Starting configuration, membrane phase separated into L_o and L_d domains enriched in saturated DPPC (green) and unsaturated DLiPC (red) lipids, respectively. Cholesterol (gray) and sugars (white) are also depicted. Water is not shown. (B) Time series of lipid mixing after the addition of 200 mM sucrose. The membrane is viewed from the top; sugars and water are not shown. Scale bars represent 5 nm. (C) Number of contacts between saturated and unsaturated lipids, normalized for the total number of lipids, after the addition of 600 mM sucrose (red diamonds), 600 mM trehalose (blue diamonds), 200 mM sucrose (red squares), 200 mM trehalose (blue squares), 100 mM sucrose (red circles), 400 mM glucose (black diamonds), and 200 mM glucose (black squares). (D) Number of contacts between saturated and unsaturated lipids, normalized for the total number of lipids, after the addition of 200 mM artificially modified sucrose, either with weaker interactions between the sugars and lipid headgroups (orange), or with a more flexible glycosidic bond between the sugar rings (purple), or with a longer glycosidic bond (magenta). The profile for normal sucrose at 200 mM is shown as reference (red).

fast, with nearly 75% of the final fraction of contacts established within 0.5 μs. We obtain similar results when we replace sucrose by another disaccharide, trehalose (Figure 1C). While the disturbing effect is observed with both disaccharides, the lateral distribution is more strongly affected by the addition of sucrose. At high sugar concentrations, 600 mM, the effect of trehalose is smaller than that of sucrose and even smaller than that of 200 mM trehalose.

Remarkably, performing the simulations with the monosaccharide glucose, the domains appear perfectly stable (Figure 1C). To make sure this difference does not arise solely from the amount of sugar rings, we compared different concentrations of monosaccharide and disaccharides containing the same moles of rings, e.g., 400 mM glucose compared to 200 mM trehalose/sucrose, and 200 mM glucose compared to 100 mM sucrose. The results indicate that even when the same number of rings is present only trehalose and sucrose are affecting the membrane organization.

dx.doi.org/10.1021/ja505476c | J. Am. Chem. Soc. 2014, 136, 16167–16175

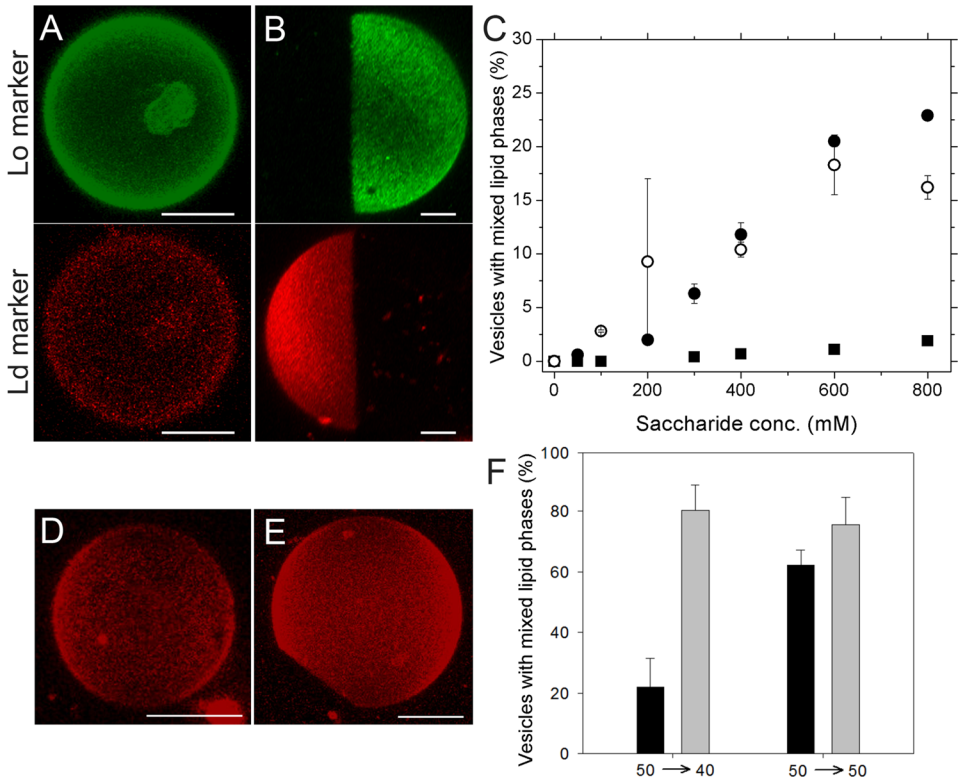

Figure 2. Domain mixing induced by saccharides in GUVs. (A) 3D projection of a GUV showing lipid mixing with the L_o and L_d domains colocalized. (B) 3D projection of a GUV with no lipid mixing, the L_o and L_d domains are segregated. Scale bars represent 2 μm. (C) Percentage of vesicles with mixed lipid phases upon addition of glucose (full squares), sucrose (full circles), and trehalose (empty circles) to SSM:DOPC:cholesterol (4:3:3) GUVs. (D) 3D projection of a GUV showing lipid mixing and (E) phase separation with only DiD as a lipid marker, scale bars represent 10 μm. (F) Percentage of vesicles with mixed lipid phases for GUVs containing a single lipid marker, the L_d marker DiD, formed at 50 °C and analyzed first at 40 °C, and then again at 50 °C (above the Tm of the lipid with the highest melting temperature). Black bars represent vesicles formed in water and gray in 400 mM sucrose. Errors represent standard deviation from two independent experiments.

Confocal Imaging Confirms the Potent Effect of Nonreducing Disaccharides on Membrane Organization. To test the *in silico* predictions, we analyzed the lipid organization of GUVs by confocal fluorescence microscopy at 20, 40, and 50 °C; the latter is above the phase transition temperature of sphingomylin, and one expects mixing of the lipids irrespective of the presence of sugars. GUVs composed of sphingomyelin (SSM), dioleoylphosphatidylcholine (DOPC), and cholesterol (4:3:3) were formed in the presence of different saccharides (see Supporting Information Figure S1 for structures of all compounds used). We quantified the disruption of the membrane organization by calculating the percentage of vesicles that show full mixing of the two lipid phases, i.e., fluorescence colocalization of L_o and L_d domains in the presence of sugars. To visualize both domains we first tested three different ways of labeling the L_o and L_d domains (see Supporting Information Methods and Figure S2). In all the experiments, we found the pair DiI-C_{18} and AF-CTB bound to the GM1 as L_d and L_o marker, respectively,[30] to be the best L_o/L_d labeling pair, i.e., when compared to DiI-C_{18} with either head- or tail-labeled GM1 (see Supporting Information Figure S2). Figure 2A,B shows an example of a vesicle with lipids from the L_o and L_d domain mixing and no mixing, respectively. The quantification of the vesicles with lipid mixing in the presence of different concentrations of glucose, sucrose, and trehalose is shown in Figure 2C. The two disaccharides, sucrose and trehalose, increased the mixing of the lipid domains more than the monosaccharide glucose did. At the highest concentration of trehalose, 800 mM, the mixing effect seems to decrease, while sucrose reaches maximum mixing at 800 mM. In line with the simulations, high concentrations of trehalose have a less disruptive effect on the membrane organization than sucrose (Figure 1C). In addition we tested glycerol, which also has no effect on the lipid organization (see Table S1 of Supporting Information).

The number of sugar rings cannot explain the remarkable effect of the disaccharides; doubling the concentration of monosaccharides would yield the same effect, and it clearly does not as shown in Supporting Information Figure S3A. The lipid mixing by 600 mM glucose is almost negligible (less than 1%) and lower than the 4.3% mixing of 300 mM sucrose. Furthermore, if we compare 300 mM sucrose with a mixture of the two monosaccharides that constitute sucrose, i.e., glucose and fructose at equal concentration, the lipid mixing is again much lower in the presence of the two monosaccharides (less than 1%). These results indicate that the linkage between the two rings of the sucrose is crucial for the effect on the membrane organization of this nonreducing disaccharide. MD simulations confirm the importance of the linkage, as discussed further below.

The fact that disaccharides are able to alter the membrane organization could be due to a change in the lipid compositions of the GUVs by the presence of the sugars during vesicle formation. To rule out this possibility, we analyzed the vesicle samples at 20 and 40 °C. We find an increased lipid phase mixing at the higher temperature with sucrose but not with

dx.doi.org/10.1021/ja505476c | J. Am. Chem. Soc. 2014, 136, 16167−16175

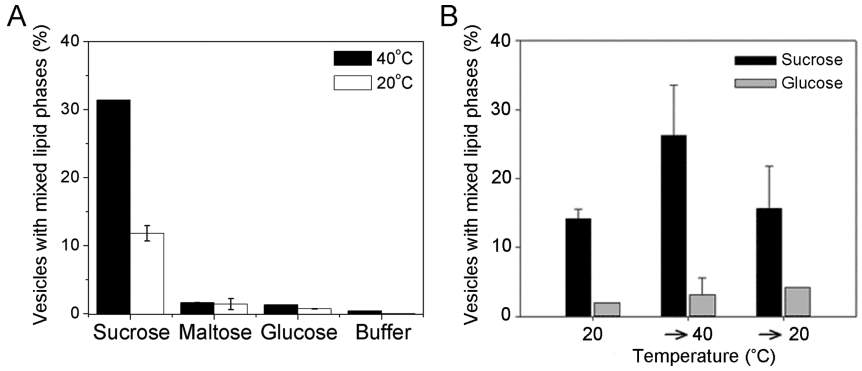

Figure 3. Temperature and lipid composition dependence of lipid phase mixing. (A) The percentage of vesicles with mixed lipid phases by sucrose, maltose, glucose, and buffer in SSM:DOPC:cholesterol (4:3:3) GUVs at 20 °C (empty bars) and 40 °C (full bars). The concentration of all sugars was 400 mM. Error bars represent standard deviations of the biological replicates. (B) Percentage of vesicles with mixed lipid phases by sucrose (black bars) or glucose (gray bars), measured consecutively at 20 °C, after heating at 40 °C and subsequently upon cooling of the vesicle sample at 20 °C. The concentration of sugars was 400 mM. Error bars represent standard deviations of technical replicates.

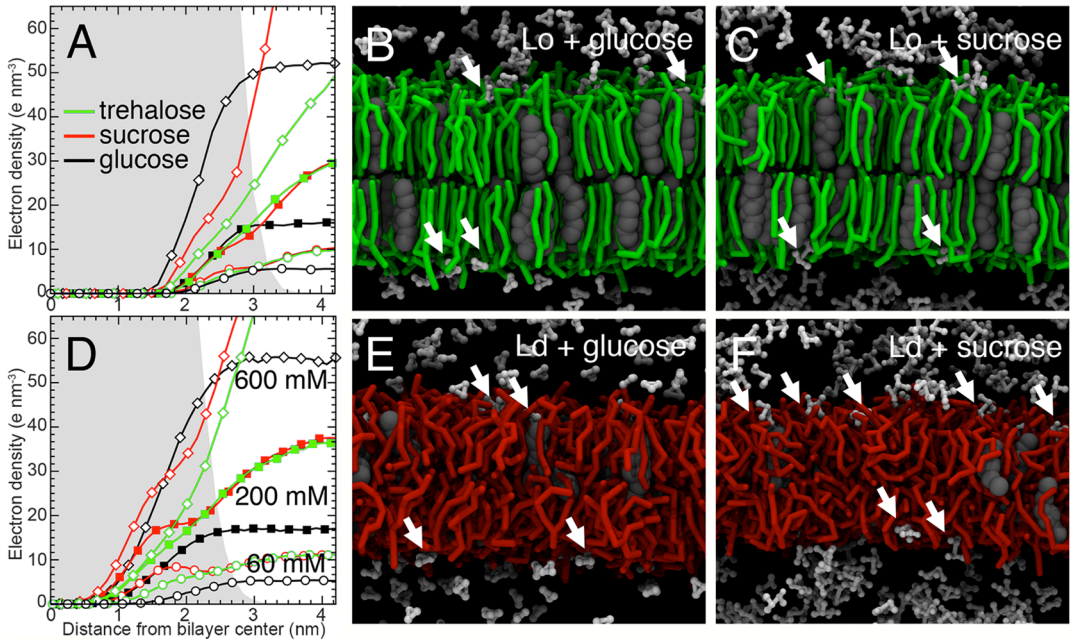

Figure 4. Interaction of L_o and L_d domains with sugars. Electron density profiles for glucose, sucrose, and trehalose interacting with L_o (A–C) or L_d (D–F) membranes. Panels A and D show a close up of the interaction between the sugars and the membrane (glucose in black, sucrose in red, and trehalose in green) at different concentrations (open circles represent 60 mM, closed squares 200 mM, and open diamonds 600 mM). The total membrane density is represented by the gray area. The average position of the lipid glycerol moiety is located at z = 2.0 nm (L_o) and z = 1.5 nm (L_d). Snapshots of the sugar distribution across the lipid–water interface for glucose interacting with L_o (B) and L_d (E); sucrose interacting with L_o (C) and L_d (F) membranes at 200 mM sugar. Interfacially embedded sugars are indicated by white arrows.

glucose, maltose, or buffer control (Figure 3A and Table S2 in Supporting Information). The experiment also shows a phase transition temperature above 40 °C for the lipid mixture SSM:DOPC:cholesterol (4:3:3), because no lipid phase mixing is observed in the control vesicles made in buffer. Next, we quantified the phase mixing of one and the same batch of vesicles at different consecutive temperatures: starting at 20 °C, then heating the sample to 40 °C, followed by cooling to 20 °C again (Figure 3B). We clearly see that the lipid phase mixing is caused by interactions of the disaccharide with the membrane rather than sugars affecting the lipid composition during vesicle formation.

The vesicle formation is very heterogeneous with not all the vesicles constituted by a ternary mixture of SSM, DOPC, and cholesterol. This observation is known to occur during GUV electroformation of ternary mixtures.[31] In all the samples we observe a substantial fraction of vesicles with only L_o or L_d staining, which we assume to be caused by the presence of predominantly one or two types of lipid (see Table S1 in Supporting Information). To increase the fraction of vesicles with both L_o and L_d domains, we formed the vesicles in water instead of phosphate buffer. To rule out possible effects on the lipid mixing by AF-CTB binding to GM1, we also analyzed the vesicles by using DiI-C_{18} only. Figure 2D,E shows an example of a vesicle with lipids from the L_o and L_d domain mixing and no mixing, respectively. In this approach of vesicle formation and domain analysis, we find a higher fraction of vesicles with distinct L_o and L_d domains, but the effect of sugars is qualitatively similar. The disaccharide sucrose induces lipid mixing when the vesicles are analyzed below the phase

dx.doi.org/10.1021/ja505476c | J. Am. Chem. Soc. 2014, 136, 16167–16175

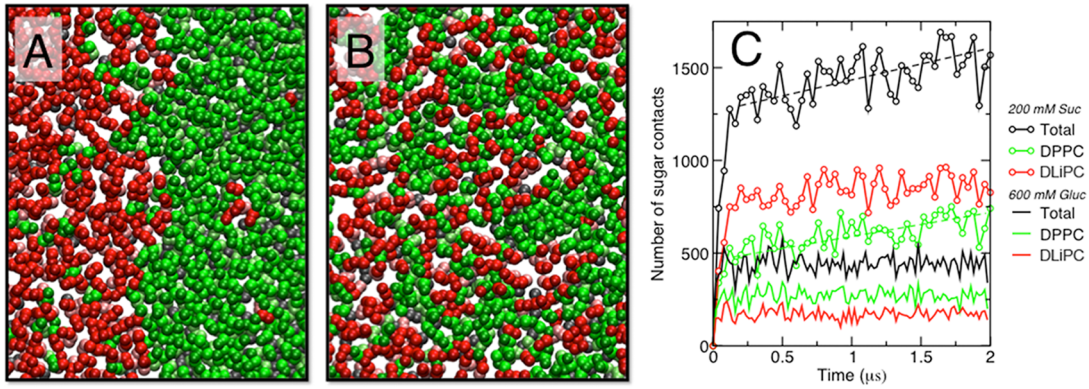

Figure 5. Surface defect hypothesis. (A, B) Top view of the initial, phase separated membrane (A) and the final mixed membrane after 2 μs upon addition of 200 mM sucrose with glycerol exposing areas ("surface defects") visible as white spots. Only headgroups (green, DPPC; red, DLiPC; gray, cholesterol) are shown. (C) Time evolution of the number of sugar–lipid contacts upon addition of 200 mM sucrose (open symbols) or 600 mM glucose (solid lines). In case of sucrose, the total number of contacts increases during mixing of the domains, in particular due to an increase in sugar–DPPC contacts (dashed lines).

transition temperature (Figure 2F); the control experiment at 50 °C shows that sucrose has little effect above the phase transition temperature of SSM. Thus, in the alternative protocol we find a higher fraction of vesicles with distinct L_o and L_d domains, and accordingly, we observe a higher fraction of vesicles with lipid mixing in the presence of sucrose. Overall, the MD simulations and experimental data are in qualitative agreement with each other.

Saccharides Interact with Lipid Headgroups in a Concentration-Dependent Manner. We have shown that disaccharides are able to modify the lateral organization of lipids in model bilayers, whereas monosaccharides do not. Moreover, the strength of the effect depends on the amount of carbohydrates in solution. A direct interaction between the sugars and lipids seems required to explain these effects. We therefore investigated the membrane surface affinity of the sugars by analyzing the electron density profiles across the membrane, obtained from additional simulations of L_o and L_d membrane mimetics. The resulting profiles are shown in Figure 4A,D; a close up of the interfacial distribution is shown in Supporting Information Figure S4. In general, we see that sugars are able to reside at the membrane–water interface up to the level of the glycerol linkage, both for L_o and L_d mimicking membranes. At higher sugar concentrations (600 mM), saturation of the interfacial sugar population is observed with a concomitant increased tendency toward clustering of the carbohydrates in the aqueous subphase. Although the absolute number of sugars at the interface still increases with increasing concentration, the relative concentration with respect to the bulk concentration decreases (Supporting Information Figure S4). Interestingly, the interfacial accumulation of sugars is more pronounced for the disaccharides, in particular in the L_d phase, whereas the L_o phase appears to accommodate glucose more easily (especially noticeable at the highest concentration of 600 mM). A graphical view of the binding mode of glucose and sucrose, at 200 mM, is shown in Figure 4B,C (L_o) and Figure 4E,F (L_d). The presence of both a membrane-bound (indicated by white arrows) and membrane-depleted population at this concentration is visible. Noticeable is the stronger embedding of the disaccharide in the L_d phase. The embedding of the interfacially bound sugars is in fact very similar to that observed in all-atom MD simulations.[32,33] Our results are also consistent with the experimental data reported by Andersen and co-workers.[25] On the basis of neutron scattering data combined with thermodynamic measurements, they show strong binding of sugars to membranes at low concentration and gradual repelling at concentrations exceeding ~200 mM when the interface is saturated.

Taken together, our results indicate that sugars are in direct contact with the phospholipid headgroups, and that this interaction is strongly affected by the amount of carbohydrates in solution. The L_d membrane favors direct interactions with disaccharides, whereas the L_o membrane interface more readily accommodates monosaccharides. However, bilayer properties such as membrane thickness or area per lipid are hardly affected by the presence of the sugars, and a destabilization of either L_d or L_o phase seems an unlikely mechanism to account for the lipid mixing.

Surface Defect Hypothesis To Account for Disaccharide Induced Lipid Mixing. Despite a stronger interfacial binding of disaccharides compared to monosaccharides, we find no clear evidence for a destabilizing effect of disaccharides on either the L_d or L_o phase. The only way to account for the disappearance of the domain segregation is, it seems, to assume stabilization of the mixed state with respect to the domain segregated state. Here, we put forward a hypothesis that would explain such an effect, involving surface defects, i.e., sites available at the interface that can accommodate a sugar molecule. The notion of surface defects is similar to the packing defects recently introduced by Vamparys et al.[34] to account for differences in membrane binding of amphipathic peptides. However, whereas in the work of Vamparys et al. packing defects were defined as local surface areas exposing part of the hydrophobic interior, here we consider more shallow defects exposing the lipid glycerol moieties. In Figure 5A we show the distribution of these surface defects (visible as white spots in the figure) in the initial, phase-separated system. A striking difference can be observed between the surface density, as well as size, of such defects in the L_d versus the L_o domain, rationalizing the increased affinity of disaccharides for the L_d phase (cf., interfacial peak of the sugar distribution, Figure 4D, Supporting Information Figure S4A). Upon domain mixing, however, the total amount of surface defects increases, as illustrated in Figure 5B. Thus, our hypothesis is that the availability of surface defects that are large enough to bind a disaccharide, a favorable interaction, drives domain mixing. If

dx.doi.org/10.1021/ja505476c | J. Am. Chem. Soc. 2014, 136, 16167–16175

this is true, one anticipates an increase in lipid−sugar contacts during domain mixing. This is indeed the case, as shown in Figure 5C.

To test our surface defect hypothesis, we performed additional MD simulations in which the pairwise interaction between the sugars and the headgroup part of the lipids was weakened (see Supporting Information Methods for details). If interfacial embedding of the disaccharides is to drive the lipid mixing, we expect to see less efficient binding of the "weakened" disaccharides, and hence a reduced driving force for domain mixing. The results, shown in Figure 1D in terms of a plot of the contact fraction between saturated and unsaturated contact lipids over time, confirm our expectation. To further test our hypothesis, we focused on the importance of the disaccharide geometry. Therefore, we performed MD simulations in which the glycosidic linker was either made longer (an increase in size from 0.429 to 1.0 nm), or made completely flexible (i.e., all the dihedral terms corresponding to the plane−plane orientation were excluded, as explained in Supporting Information Methods). The effect of these changes in disaccharide geometry on lipid mixing is shown in Figure 1D in the case of 200 mM sucrose. Remarkably, sucrose in which the two monomers are linked at a larger distance is unable to disperse the domains. Keeping the linkage at the natural distance but increasing its flexibility, on the other hand, results in fast mixing of the lipids. The magnitude of the domain disruption and lipid remixing is even larger compared to normal sucrose.

We conclude that the close proximity of two sugar rings, a distinguishing feature of disaccharides, causes the destabilization of L_o/L_d coexistence via a mechanism involving surface defects. The amount of surface defects that can accommodate a disaccharide is optimized in the mixed state, providing the driving force for domain mixing.

Membrane Organization Is Exclusively Altered by Nonreducing Sugars. We show that sucrose and trehalose affect the lipid organization of the membranes, whereas glucose does not. Our *in silico* data suggest that the presence of two sugar rings linked closely together is a prerequisite for this effect. To further prove that we need disaccharides to disrupt the membrane organization, we checked other disaccharides with our experimental setup. Surprisingly, none of the disaccharides tested (palatinose, gentiobiose, and maltose) have an actual effect on mixing the lipid domains at 400 mM (Supporting Information Figure S3B). As opposed to sucrose and trehalose, which are nonreducing disaccharides, these disaccharides are reducing sugars. In solution, reducing sugars can have one of the monosaccharide rings (reducing ring) open containing an aldehyde group, which is in equilibrium with the hemiacetal (when the pyranose ring is formed) and can act as a reducing agent. In order to verify whether the lack of lipid mixing of the reducing sugars is due to the opening of the hemiacetal to aldehyde, we analyzed two analogues of maltose, maltitol, and methyl-maltoside (see structures in Supporting Information Figure S1). Maltitol is a hydrogenated maltose and does not possess an aldehyde in its open form, so the reaction back to the hemiacetal (closed pyranose) is not possible, giving rise to a fully open ring. In contrast to maltitol, methyl-maltoside has an extra methyl group in the hydroxyl of the hemiacetal, eliminating the equilibrium toward the aldehyde and locking the saccharide in its closed form. As shown in Supporting Information Figure S3B, maltitol acts similarly to the regular maltose, having a low effect on lipid mixing. On the contrary, methyl-maltoside causes a significant increase in the percentage of vesicles with lipid phase mixing. These results show that only disaccharides containing two closed rings, either the two nonreducing (sucrose and trehalose) or the synthetic maltose analogue methyl-maltoside, are able to disrupt the lipid organization.

To test whether the ring opening of the reducing saccharides is favored upon binding to the lipid bilayer, we performed measurements of maltose in solution and in the presence of the SSM:DOPC:cholesterol (4:3:3) bilayer using solid-state NMR spectroscopy (ssNMR). We compared ^{13}C ssNMR spectra of maltose in solution, and in the presence of membranes (Supporting Information Figure S5A). In the latter case, a reference spectrum, using dipolar CP transfers that are most sensitive to rigid molecular components, was dominated by lipid signals. This observation implies that maltose remains loosely associated with the membrane and allowed us to concentrate on spectral regions characteristic of maltose ring positions. In this spectral region, we observed small chemical shift changes for the anomeric carbons of maltose (Supporting Information Figure S5A). Second, we detected an additional peak at 81.0 ppm which resonates downfield of the fourth position of maltose (80.0 ppm) in line with the ^{13}C spectrum of maltitol (85.1 ppm) in which the reducing ring is irreversibly opened (Supporting Information Figure S5B).

Taken together, the NMR measurements provide qualitative evidence that there is a change in the maltose structure in the presence of membranes. We speculate that a significant fraction of maltose has the reducing ring in an open form in the presence of membranes, which might be the reason that maltose is not able to disrupt the membrane organization. Our work thus indicates that not all disaccharides are able to disturb the membrane organization. The closed conformation of the second monosaccharide ring is a key factor in the lipid mixing. Among all saccharides tested, the nonreducing sugars sucrose and trehalose are the only two capable of reorganizing the lipids of the membranes.

■ DISCUSSION

The picture emerging from our combined computational and experimental approach is the following. Mono- and disaccharides interact with the lipid membrane by direct interactions of the carbohydrates with the phospholipid headgroups as shown by the MD simulations. These interactions affect the organization of lipid domains present in membranes formed by saturated lipids, unsaturated lipids, and cholesterol. The extent of lipid mixing is directly related to the amount of sugar present in solution. However, the disruptive properties are exclusive to nonreducing disaccharides such as sucrose and trehalose, which insert quite deeply at the membrane/water interface when compared to glucose. Moreover, sucrose and trehalose are composed of two pyranoses without a free hemiacetal. Those disaccharides are much bulkier and require more space to fit in between the lipid headgroups. We show that interfacial spaces, or sites, to accommodate the disaccharides are more abundant in the disordered state, and hence provide a driving force for disappearance of the L_o phase as formulated by our surface defect hypothesis. In other words, both the L_d and the mixed phase exhibit defects to which disaccharides can bind and thus lower the free energy. Any membrane area taken up by an L_o phase is "wasted" for this effect. This shifts the balance away from demixing. Thus, the disaccharides promote mixing by lowering the free energy of

the mixed state. Monosaccharides, on the other hand, are small enough to even fit in the surface defects present in the ordered domains. Reducing sugars, once they are bound to the lipids, might be stabilized in the open form where only the first pyranose ring is present. This conformation might not be bulky enough to require lipid mixing, i.e., essentially they behave as a monosaccharide. Reducing sugars change their structure in water almost without any energy loss, so opening the reducing ring does not require a lot of energy. There is no quantitative data available about the opening and closing of reducing sugars in the presence of membranes, but the observations of maltose and maltitol opposed to those of methyl-maltoside in the lipid mixing together with the structural observations by ssNMR support this hypothesis.

The MD simulations and the experimental observations are in qualitative agreement, even though the level of mixing observed in the experiments (up to 25%) is lower than what is seen in the simulations (effectively 100% mixing). However, it is important to keep in mind the limitations of the simulation setup. First of all, to be able to observe domain mixing, a coarse-grain model was used. Although our specific model has been validated with respect to a large variety of both experimental data and results from all-atom simulations (see Supporting Information), eventually our predictions should be reproduced using more detailed models. One of the main limitations in the representation of sugars, as well as the aqueous solvent, is the loss of the directionality of hydrogen bonds. Within the resolution of the Martini model, hydrogen bonds are necessarily isotropically averaged. Interestingly, the H-bond directionality does not seem to play a major role in reproducing the key experimental findings, in particular the behavior of mono- versus disaccharides. The disordered nature of the membrane/water interface likely accounts for the decreased importance of H-bond directionality compared to overall H-bonding strength. Nevertheless, capturing the subtle differences between sucrose and trehalose is challenging. Furthermore, to make the simulations feasible, the *in silico* membranes are limited in size to the nanometer length scale. Domain mixing on this scale cannot be quantitatively compared to domain mixing on the scale of full liposomes, as probed experimentally. Importantly, the qualitative trends of lipid mixing as a function of sugar type are in agreement. Another difference is that, in the initial experiments, the L_o phase was composed of a different type of saturated lipid. The MD simulations were performed with DPPC, whereas in the experiments SSM was used. A control experiment showed the same behavior on lipid mixing by sucrose, maltose, and glucose with membranes composed of DPPC instead of SSM (Figure S3C and Supporting Information Table S3). Finally, we emphasize that vesicles with L_o and L_d staining have the three types of lipids, but the ratio of SSM:DOPC:cholesterol can vary among the vesicles. We attribute the incomplete lipid phase mixing in the experiments to heterogeneity in the lipid composition of the vesicles, which precludes quantitative comparisons with the MD simulations.

We note that nematodes, embryonic cysts of crustaceans and yeast/fungi, can accumulate high amounts of trehalose up to 30% of their dry weight, which is equivalent to concentrations in the molar range. The nonreducing sugars sucrose and trehalose are the only two saccharides known to accumulate in molar amounts by numerous organisms under conditions of complete dehydration.[35,36] Sugars like trehalose are also synthesized or taken up under conditions of osmotic stress (partial dehydration), in which case the cytoplasmic levels are in the submolar range.[37] It is well-accepted that these sugars may replace the water molecules around the polar residues of membranes and proteins. This stabilizes the membranes by avoiding the shrinkage, lateral stress, and the increase in the phase transition temperature when water is removed in the process of drying.[38] Here, we add the possibility that sucrose and trehalose prevent membrane phase separation. If these sugars have similar effects on the structure of native membranes, then the synthesis or accumulation of nonreducing disaccharides might dissolve the nanoscale assemblies present in the plasma membrane of eukaryotes, which may impact the functioning of several membrane proteins. The change in the membrane lipid environment could affect the function and more importantly the stability of proteins, which is likely to be critical during anhydrobiosis. This membrane domain destabilization effect could be a more general mechanism of action of membrane-active compounds including anesthetics, phytochemicals, and amphiphilic drugs. A comprehensive study on a large array of small hydrophobic molecules, lowering critical mixing temperatures in plasma membrane vesicles, corroborates this idea[39] and provides a possible general mechanism for anesthetic action.[40] Hydrophobic compounds in general were found to reshape membrane domains, with aromatic ones stabilizing, and aliphatic compounds destabilizing, domains.[41] Vitamin E, an example of an amphipathic compound, has been shown to decrease the tendency to form domains in ternary model membrane systems.[42] Alcohols, including benzyl alcohol and ethanol, were also found to destabilize ordered membrane domains.[43,44] Similarly, a series of 2-hydroxyfatty acid derivatives affects lipid mixing and the localization and activity of membrane proteins involved in signaling cascades.[45] Taken together, there is growing evidence for the role of membrane active compounds as powerful modulators of cell response through lateral membrane reorganization.

METHODS

Molecular Dynamics Simulations. All simulations were carried out with the Gromacs MD package, version 4.0.5. The MARTINI coarse grained (CG) force field for lipids[46,47] was used to describe the interactions. The MARTINI model has been previously applied to study a variety of ternary membrane systems,[48−50] including sugar−membrane interactions.[51] For an elaborate discussion on the limitations of the MARTINI model we refer to Marrink and Tieleman;[28] validation of the parameters used in the current study is discussed in the Supporting Information. Molecules considered here are the saturated lipids dipalmitoyl-phosphatidylcholine (DPPC), the unsaturated lipid dilinoleoyl-PC (DLiPC), cholesterol, and the sugars glucose, trehalose, and sucrose at a range (60−600 mM) of concentrations. An equilibrated L_o/L_d lipid bilayer was used as initial configuration for our simulations. The system is composed of 769 DPPC, 507 DLiPC, and 538 cholesterol molecules (4:3:3 molar ratio). Additional simulations of L_o and L_d mimetic membranes were used to probe the structural effects of sugar binding. The L_o membrane consists of 328 DPPC and 164 cholesterol molecules (2:1 ratio), the L_d membrane of 448 DLiPC and 44 cholesterols (10:1 ratio). Temperature in each case was maintained by coupling to a heat bath at 288 K. More details are given in the Supporting Information.

GUVs Preparation. GUVs were prepared by electroformation.[52,53] Briefly, a lipid mixture of *N*-stearoyl-D-*erythro*-sphingosylphosphorylcholine (SSM), 1,2-dioleoyl-*sn*-glycero-3-phosphocholine (DOPC), and cholesterol was prepared from the lipid stock solution in chloroform/methanol (9:1) with a molar ratio of 4:3:3 (lipids were purchased from Avanti Polar Lipids). The fluorescent lipid marker DiI-C_{18} (1,1′-dioctadecyl-3,3,3′,3′-tetramethylindodicarbocyanine perchlorate, Molecular Probes, Invitrogen) dissolved in chloroform, and the

dx.doi.org/10.1021/ja505476c | J. Am. Chem. Soc. 2014, 136, 16167−16175

ovine brain ganglioside GM1 (GM1, Avanti Polar Lipids) dissolved in methanol:H_2O (1:1) were added to the lipid mixture at the amount of 0.1 mol %. The lipid mixture was applied to indium-tin-oxide-coated glasses, solvents were evaporated, and glasses were prewarmed at 50 °C before placing them in the electroformation chamber of Nanion Vesicle Prep Pro (Nanion Technologies GmbH, Munich, Germany). The chamber was filled with buffer (10 mM KPi, pH 7.2) or water, or buffer or water containing different concentrations of saccharides, prewarmed at 50 °C. An alternating current was applied across the cell unit with 1.1 V, 10 kHz of frequency, and 50 °C for 1 h. Sugar solutions osmolarities were checked on OSMOMAT 030 (Genotec). GUVs had a diameter of 5−15 μm. As a control we repeated some of the experiments with DPPC instead of SSM similar to the MD simulations (data shown in Supporting Information Figure S3C and Table S3).

Confocal Fluorescence Microscopy and Data Analysis. GUVs were incubated for 10 min with the Alexa Fluor 488 conjugate of cholera toxin B subunit (AF-CTB, Molecular Probes, Invitrogen), for which GM1 is the natural receptor; the complex GM1-CTB was detected only in areas from which DiI-C_{18} was strongly excluded.[54] Thus, AF-CTB reports SSM-enriched (L_o) domains and DiI-C_{18} reports DOPC-enriched domains. After incubation, GUVs were immobilized with the hydrogel ArtiCYT (Nano-FM), previously adjusted to the desired saccharide concentration to avoid osmotic stress. Samples were imaged on a commercial laser-scanning confocal microscope, LSM 710 (Carl Zeiss MicroImaging, Jena, Germany), using an objective C-Apochromat 40×/1.2NA, a blue argon ion laser (488 nm), and a red He−Ne laser (633 nm) at 20 or 40 °C. The pixel dwell time for the laser-scanning was 2.55 μs with a pixel step of 0.2 μm. Images were collected from at least two independent lipid preparations (biological replicates) for each sugar concentration, and each preparation was analyzed three times (technical replicates). A total of 500 GUVs were analyzed from randomly chosen images of each sugar concentration. GUVs were classified in four categories: mixed (where the probes of the liquid-ordered and disordered phases colocalize), separated (where the two probes are localized in different domains), red (vesicles stained with DiI-C_{18} and reporting the liquid-disordered phase), or green (vesicles stained with AF-CTB and reporting the liquid-ordered phase). The purely red and green vesicles are likely due to the heterogeneity in the GUV formation; i.e., not all the vesicles constitute a ternary mixture of SSM, DOPC, and cholesterol as observed by Kahya and co-workers for the same vesicles.[30] For each concentration, weighted averages and standard deviations were calculated (considering the number of GUVs per image) for the technical replicates and for the biological replicates. The percentages of vesicles with lipid phase mixing were also calculated considering only vesicles with ternary mixture of lipids by omitting the red and green vesicles. These effective percentages were plotted in the all the figures and are shown together with the rest of the statistics in Table S1 of Supporting Information. The standard deviation of the percentage of vesicles of a given category varies, in particular when the fraction is low. Taking the data as a whole we estimate the uncertainty in the measurements to be on the order of 20% of the value presented.

■ ASSOCIATED CONTENT

Supporting Information

Materials and methods details, 5 figures, and 4 tables. This material is available free of charge via the Internet at http://pubs.acs.org.

■ AUTHOR INFORMATION

Corresponding Authors

b.poolman@rug.nl

s.j.marrink@rug.nl

Author Contributions

G.M. and C.A.L. contributed equally to this work.

Notes

The authors declare no competing financial interest.

■ ACKNOWLEDGMENTS

This work was supported by The Netherlands Organisation for Scientific Research (NWO): ECHO.08.BM.041 and Chem-Them "Out-of-Equilibrium Self-Assembly" 728.011.202). A.C. was supported by NWO (VICI grant 700.11.344 to M.B.). The authors thank Manuel Jäger for kindly providing us with the methyl-maltoside, Adri Minnaard and Katja Loos for help with the interpretation of the NMR data and Nano-FM for the ArtiCYT donation.

■ REFERENCES

(1) Andrews, S. S.; Addy, N. J.; Brent, R.; Arkin, A. P. *PLoS Comput. Biol.* **2010**, *6*, e1000705.

(2) Crowe, L. M. *Comp. Biochem. Physiol., Part A: Mol. Integr. Physiol.* **2002**, *131*, 505.

(3) Clegg, J. S. *Comp. Biochem. Physiol., Part B: Biochem. Mol. Chem.* **2001**, *128*, 613.

(4) Crowe, J. H.; Oliver, A. E.; Tablin, F. *Integr. Comp. Biol.* **2002**, *42*, 497.

(5) Rebecchi, L.; Altiero, T.; Guidetti, R. *Invertebr. Surv. J.* **2007**, *4*, 65.

(6) Crowe, J. H.; Crowe, L. M.; Carpenter, J. F.; Aurell Wistrom, C. *Biochem. J.* **1987**, *242*, 1.

(7) Cacela, C.; Hincha, D. K. *Biophys. J.* **2006**, *90*, 2831.

(8) Oliver, A. E.; Kendall, E. L.; Howland, M. C.; Sanii, B.; Shreve, A. P.; Parikh, A. N. *Lab Chip* **2008**, *8*, 892.

(9) Ohtake, S.; Schebor, C.; de Pablo, J. J. *Biochim. Biophys. Acta* **2006**, *1758*, 65.

(10) Koster, K. L.; Webb, M. S.; Bryant, G.; Lynch, D. V. *Biochim. Biophys. Acta* **1994**, *1193*, 143.

(11) Lenné, T.; Garvey, C. J.; Koster, K. L.; Bryant, G. *J. Phys. Chem. B* **2009**, *113*, 2486.

(12) Tsvetkova, N. M.; Phillips, B. L.; Crowe, L. M.; Crowe, J. H.; Risbud, S. H. *Biophys. J.* **1998**, *75*, 2947.

(13) Lenné, T.; Bryant, G.; Holcomb, R.; Koster, K. L. *Biochim. Biophys. Acta* **2007**, *1768*, 1019.

(14) Crowe, J. H.; Crowe, L. M.; Wolkers, W. F.; Oliver, A. E.; Ma, X.; Auh, J.-H.; Tang, M.; Zhu, S.; Norris, J.; Tablin, F. *Integr. Comp. Biol.* **2005**, *45*, 810.

(15) Nakagaki, M.; Nagase, H.; Ueda, H. *J. Membr. Sci.* **1992**, *73*, 173.

(16) Crowe, J. H.; Crowe, L. M.; Carpenter, J. F.; Rudolph, A. S.; Wistrom, C. A.; Spargo, B. J.; Anchordoguy, T. J. *Biochim. Biophys. Acta* **1988**, *947*, 367.

(17) Crowe, J. H.; Hoekstra, F. A.; Crowe, L. M. *Annu. Rev. Physiol.* **1992**, *54*, 579.

(18) Horta, B. A. C.; Perić-Hassler, L.; Hünenberger, P. H. *J. Mol. Graphics Modell.* **2010**, *29*, 331.

(19) Green, J. L.; Angell, C. A. *J. Phys. Chem.* **1989**, *93*, 2880.

(20) Massari, A. M.; Finkelstein, I. J.; McClain, B. L.; Goj, A.; Wen, X.; Bren, K. L.; Loring, R. F.; Fayer, M. D. *J. Am. Chem. Soc.* **2005**, *127*, 14279.

(21) Westh, P. *Phys. Chem. Chem. Phys.* **2008**, *10*, 4110.

(22) Crowe, J. H.; Whittam, M. A.; Chapman, D.; Crowe, L. M. *Biochim. Biophys. Acta* **1984**, *769*, 151.

(23) Lambruschini, C.; Relini, A.; Ridi, A.; Cordone, L.; Gliozzi, A. *Langmuir* **2000**, *16*, 5467.

(24) Van Den Bogaart, G.; Hermans, N.; Krasnikov, V.; de Vries, A. H.; Poolman, B. *Biophys. J.* **2007**, *92*, 1598.

(25) Andersen, H. D.; Wang, C.; Arleth, L.; Peters, G. H.; Westh, P. *Proc. Natl. Acad. Sci. U.S.A.* **2011**, *108*, 1874.

(26) Lingwood, D.; Simons, K. *Science* **2010**, *327*, 46.

(27) Simons, K.; Sampaio, J. L. *Cold Spring Harbor Perspect. Biol.* **2011**, *3*, a004697.

(28) Marrink, S. J.; Tieleman, D. P. *Chem. Soc. Rev.* **2013**, *42*, 6801.

(29) Veatch, S. L.; Keller, S. L. *Biophys. J.* **2003**, *85*, 3074.

(30) Kahya, N.; Scherfeld, D.; Bacia, K.; Poolman, B.; Schwille, P. *J. Biol. Chem.* **2003**, *278*, 28109.

(31) Betaneli, V.; Worch, R.; Schwille, P. *Chem. Phys. Lipids* **2012**, *165*, 630.
(32) Pereira, C. S.; Hünenberger, P. H. *Mol. Simul.* **2008**, *34*, 403.
(33) Kapla, J.; Wohlert, J.; Stevensson, B.; Engström, O.; Widmalm, G.; Maliniak, A. *J. Phys. Chem. B* **2013**, *117*, 6667.
(34) Vamparys, L.; Gautier, R.; Vanni, S.; Bennett, W. F. D.; Tieleman, D. P.; Antonny, B.; Etchebest, C.; Fuchs, P. F. J. *Biophys. J.* **2013**, *104*, 585.
(35) Hengherr, S.; Heyer, A. G.; Köhler, H.-R.; Schill, R. O. *FEBS J.* **2008**, *275*, 281.
(36) Sebollela, A.; Louzada, P. R.; Sola-Penna, M.; Sarone-Williams, V.; Coelho-Sampaio, T.; Ferreira, S. T. *Int. J. Biochem. Cell Biol.* **2004**, *36*, 900.
(37) Kempf, B.; Bremer, E. *Arch. Microbiol.* **1998**, *170*, 319.
(38) Crowe, J. H.; Carpenter, J. F.; Crowe, L. M. *Annu. Rev. Physiol.* **1998**, *60*, 73.
(39) Gray, E.; Karslake, J.; Machta, B. B.; Veatch, S. L. *Biophys. J.* **2013**, *105*, 2751.
(40) Turkyilmaz, S.; Chen, W.-H.; Mitomo, H.; Regen, S. L. *J. Am. Chem. Soc.* **2009**, *131*, 5068.
(41) Barnoud, J.; Rossi, G.; Marrink, S. J.; Monticelli, L. *PLOS Comp. Biol.* **2014**, *10*, e1003873.
(42) Muddana, H. S.; Chiang, H. H.; Butler, P. J. *Biophys. J.* **2012**, *102*, 489.
(43) Marquês, J. T.; Viana, A. S.; de Almeida, R. F. M. *Biochim. Biophys. Acta* **2011**, *1808*, 405.
(44) Maula, T.; Westerlund, B.; Slotte, J. P. *Biochim. Biophys. Acta* **2009**, *1788*, 2454.
(45) Ibarguren, M.; López, D. J.; Encinar, J. A.; González-Ros, J. M.; Busquets, X.; Escribá, P. V. *Biochim. Biophys. Acta* **2013**, *1828*, 2553.
(46) Marrink, S. J.; Risselada, H. J.; Yefimov, S.; Tieleman, D. P.; de Vries, A. H. *J. Phys. Chem. B* **2007**, *111*, 7812.
(47) López, C. A.; Rzepiela, A. J.; de Vries, A. H.; Dijkhuizen, L.; Hünenberger, P. H.; Marrink, S. J. *J. Chem. Theory Comput* **2009**, *5*, 3195.
(48) Risselada, H. J.; Marrink, S. J. *Proc. Natl. Acad. Sci. U.S.A.* **2008**, *105*, 17367.
(49) Domański, J.; Marrink, S. J.; Schäfer, L. V. *Biochim. Biophys. Acta* **2012**, *1818*, 984.
(50) Bennett, W. F. D.; Tieleman, D. P. *Biochim. Biophys. Acta* **2013**, *1828*, 1765.
(51) López, C. A.; de Vries, A. H.; Marrink, S. J. *Sci. Rep.* **2013**, *3*, 2071.
(52) Dimitrov, D. S.; Angelova, M. I. *J. Electroanal. Chem.. Interfacial Electrochem.* **1988**, *253*, 323.
(53) Angelova, M. I.; Dimitrov, D. S. *Faraday Discuss. Chem. Soc.* **1986**, *81*, 303.
(54) Hammond, A. T.; Heberle, F. A.; Baumgart, T.; Holowka, D.; Baird, B.; Feigenson, G. W. *Proc. Natl. Acad. Sci. U.S.A.* **2005**, *102*, 6320.